AJNR

Compressed Sensitivity Encoding Artificial Intelligence Accelerates Brain Metastasis Imaging by Optimizing Image Quality and Reducing Scan Time

Mengmeng Wang, Yue Ma, Linna Li, Xingchen Pan, Yafei Wen, Ying Qiu, Dandan Guo, Yi Zhu, Jianxiu Lian and Dan Tong

AJNR Am J Neuroradiol 2024, 45 (4) 444-452
doi: https://doi.org/10.3174/ajnr.A8161
http://www.ajnr.org/content/45/4/444

Compressed Sensitivity Encoding Artificial Intelligence Accelerates Brain Metastasis Imaging by Optimizing Image Quality and Reducing Scan Time

Mengmeng Wang, Yue Ma, Linna Li, Xingchen Pan, Yafei Wen, Ying Qiu, Dandan Guo, Yi Zhu, Jianxiu Lian, and Dan Tong

ABSTRACT

BACKGROUND AND PURPOSE: Accelerating the image acquisition speed of MR imaging without compromising the image quality is challenging. This study aimed to evaluate the feasibility of contrast-enhanced (CE) 3D T1WI and CE 3D-FLAIR sequences reconstructed with compressed sensitivity encoding artificial intelligence (CS-AI) for detecting brain metastases (BM) and explore the optimal acceleration factor (AF) for clinical BM imaging.

MATERIALS AND METHODS: Fifty-one patients with cancer with suspected BM were included. Fifty participants underwent different customized CE 3D-T1WI or CE 3D-FLAIR sequence scans. Compressed SENSE encoding acceleration 6 (CS6), a commercially available standard sequence, was used as the reference standard. Quantitative and qualitative methods were used to evaluate image quality. The SNR and contrast-to-noise ratio (CNR) were calculated, and qualitative evaluations were independently conducted by 2 neuroradiologists. After exploring the optimal AF, sample images were obtained from 1 patient by using both optimized sequences.

RESULTS: Quantitatively, the CNR of the CS-AI protocol for CE 3D-T1WI and CE 3D-FLAIR sequences was superior to that of the CS protocol under the same AF ($P < .05$). Compared with reference CS6, the CS-AI groups had higher CNR values (all $P < .05$), with the CS-AI10 scan having the highest value. The SNR of the CS-AI group was better than that of the reference for both CE 3D-T1WI and CE 3D-FLAIR sequences (all $P < .05$). Qualitatively, the CS-AI protocol produced higher image quality scores than did the CS protocol with the same AF (all $P < .05$). In contrast to the reference CS6, the CS-AI group showed good image quality scores until an AF of up to 10 (all $P < .05$). The CS-AI10 scan provided the optimal images, improving the delineation of normal gray-white matter boundaries and lesion areas ($P < .05$). Compared with the reference, CS-AI10 showed reductions in scan time of 39.25% and 39.93% for CE 3D-T1WI and CE 3D-FLAIR sequences, respectively.

CONCLUSIONS: CE 3D-T1WI and CE 3D-FLAIR sequences reconstructed with CS-AI for the detection of BM may provide a more effective alternative reconstruction approach than CS. CS-AI10 is suitable for clinical applications, providing optimal image quality and a shortened scan time.

ABBREVIATIONS: AF = acceleration factor; BM = brain metastases; CE = contrast-enhanced; CNR = contrast-to-noise ratio; CS = compressed SENSE; AI = artificial intelligence; SENSE = sensitivity encoding

In recent years, with the prolonged survival of patients with cancer, the incidence of brain metastases (BM) has increased substantially, and BM have become the most common intracranial tumors in adults.[1,2] BM have an important impact on the TNM-staging and clinical therapy of tumors. In addition, the number and size of BM are closely related to the choice of treatment method (eg, stereotactic radiosurgery versus surgical excision).[3] Therefore, the early detection and accurate diagnosis of BM are vital.[4]

With its excellent soft tissue contrast and high-resolution imaging capabilities, contrast-enhanced (CE) MR imaging has emerged as the primary imaging technique for screening and diagnosing BM. According to studies by Kaufmann et al,[1] CE-T1WI sequences can provide high-contrast images and information on the location, morphology, and blood supply of BM. CE-FLAIR sequences have better visibility of leptomeningeal metastases and superficial cortical metastases. Moreover, 3D MR imaging scanning is more sensitive than 2D scanning, and it offers the advantage of being able to detect small BM.[5,6] However, the time-consuming image

Received October 11, 2023; accepted after revision December 25.

From the Department of Radiology (M.W., Y.M., L.L., X.P., Y.W., Y.Q., D.G., D.T.), The First Hospital of Jilin University, Changchun, China; and Philips Healthcare (Y.Z., J.L.), Beijing, China.

Mengmeng Wang and Yue Ma contributed equally to the work.

Grant Support: This work was supported by grants from the Jilin Provincial Department of Finance (Correction: Nos. JLSWSRCZX2021-2).

Please address correspondence to Dan Tong, Department of Radiology, The First Hospital of Jilin University, Changchun 130000, China; e-mail: tongdan@jlu.edu.cn

http://dx.doi.org/10.3174/ajnr.A8161

acquisition of 3D sequences can limit clinical applications under certain circumstances, especially in patients who cannot remain stationary for a long time due to pain or a disturbance of consciousness.[7]

Accelerating the image acquisition speed of MR imaging without reducing the image quality has always been challenging. Several image acquisition and postprocessing technologies have been developed over the past few decades, with 2 of the more influential developments being parallel imaging and compressed sensing.[8] In particular, compressed sensitivity encoding (CS), based on the principle of compressed sensing and the commonly used sensitivity encoding (SENSE) technology, has been used to optimize MR imaging scanning sequences of the brain, liver, and nerves.[9-11] CS implements random undersampling in *k*-space and capitalizes on the sparsity of signals during reconstruction. By using wavelet transforms, CS distinguishes between signal and noise. This strategy allows CS to accelerate the imaging process by operating at a sampling rate obviously lower than that prescribed by the Nyquist sampling theorem, and this enables the reconstruction of complete signals from limited data, reducing the acquisition time without compromising the SNR, especially at higher acceleration factors (AFs).[12] Compared with traditional acquisition, CS was shown to reduce the acquisition time of 3D T1-echo-spoiled gradient-echo and 3D T2-FLAIR sequences for brain tumors by 35% (2:56 minutes versus 4:43 minutes) and 25% (3:36 minutes versus 4:33 minutes), respectively, without sacrificing image quality.[7] Integrating artificial intelligence (AI) into MR imaging reconstruction has recently attracted considerable attention to the further acceleration of the scan speed.[13,14] CS-AI is a novel reconstruction algorithm that applies an adaptive CS network approach inspired by CS theory to reconstruct images, builds on the iterative shrinkage-thresholding algorithm (ISTA)-Net framework developed by Zhang et al,[15] and introduces strong prior information. It has demonstrated superior performance in reconstructing images from highly undersampled *k*-space data, improving the speed and quality of the reconstruction.[16]

To further improve the image scanning sequences of BM, we applied CS-AI technology to prospectively scan patients to achieve a balance between shortening the scanning time and improving the image quality. Therefore, the purposes of this study were to acquire highly accelerated CE 3D-T1WI and CE 3D-FLAIR images by using CS-AI framework reconstruction and to evaluate the image quality of CS-AI with different and high AFs, compared with those of the CS technique, to explore the optimal AF for the clinical imaging of BM.

MATERIALS AND METHODS

This prospective study was approved by our institution's review board (ID: 22K036-001), and written informed consent was obtained from all participants.

Patient Selection

From January to November 2022, we recruited 60 patients with cancer with suspected BM for brain MR imaging examinations. Five patients who exhibited BM disappearance and 4 patients with severe imaging artifacts were excluded from the study. The criteria for determining BM are as follows: 1) new enhanced lesions, increased size of existing lesions on follow-up CE MR imaging, or decreased size or disappeared lesions after treatment; 2) lesions that were not artifacts or normally enhanced structures; and 3) enhanced lesions occurring in the brain parenchyma.[5] Finally, 51 patients (25 patients each in the CE 3D-T1WI and CE 3D-FLAIR groups and 1 patient in the ultimate optimized sequences group) were enrolled.

Image Acquisition

All MR images of the patients were obtained by using a 3T MR scanner (Ingenia Elition, Philips Healthcare) with 16-channel head coils. The patients underwent a conventional MR imaging examination, including 2D-T1WI, 2D-T2WI, 2D T2-FLAIR, and DWI sequences. Enhanced scans were initiated 3 minutes after a single dose of gadolinium contrast injection (0.1 mmol/kg Gadovist at a rate of 1.0 mL/s). A timing bolus was used to determine the precise onset of imaging post contrast administration. Twenty-five patients underwent customized CE 3D-T1WI (3D BrainVIEW T1-weighted TSE, Philips Healthcare) sequence scanning, whereas another 25 patients received customized CE 3D-FLAIR (3D BrainVIEW FLAIR) sequence scanning (Fig 1). For these sequences, we only altered the AF and the reconstruction methods (CS or CS-AI); all other scanning parameters remained unchanged. In addition, to account for the impact of contrast agent concentration decay, the order of AFs (ranging from 6 to 12) used during the data acquisition was randomized. The denoising level of the CS group was set to "system default," and the CS-AI group was set to "complete." The thin section sagittal images that could be 3D-reconstructed were obtained. The parameters of the MR scanning are summarized in Tables 1 and 2.

CS-AI Algorithm

CS-AI reconstruction is an "adaptive CS network" based on deep learning and inspired by CS theory.[15] CS-AI replaces the iterative optimization process and the traditional wavelet transform in CS with a convolutional neural network to deal with undersampled *k*-space data. The algorithm combines a multiscale sparse method based on learning with the compressed sensing reconstruction method to ensure data consistency.[17] The algorithm also integrates prior information, such as the phase constraint and image background, and uses a deep neural network to refine and modify previous assumptions. The CS-AI was trained on approximately 740,000 MR images (1.5T and 3T) of various anatomic regions and imaging contrasts.[16] Its performance is better than the traditional CS reconstruction algorithm and deep learning reconstruction algorithms that do not consider prior knowledge.[16,18,19]

Imaging Evaluation

Quantitative and qualitative image analysis methods were applied to evaluate the image quality of the CE 3D-T1WI and CE 3D-FLAIR sequences that were reconstructed by using CS and CS-AI with different AFs (6–12). All images were transmitted and reconstructed by using a picture archiving communication system and an IntelliSpace Portal (V9; Philips Healthcare).

Quantitative Image Analysis. Two radiologists (Y.F. and M.W.) with more than 8 years of experience performed quantitative

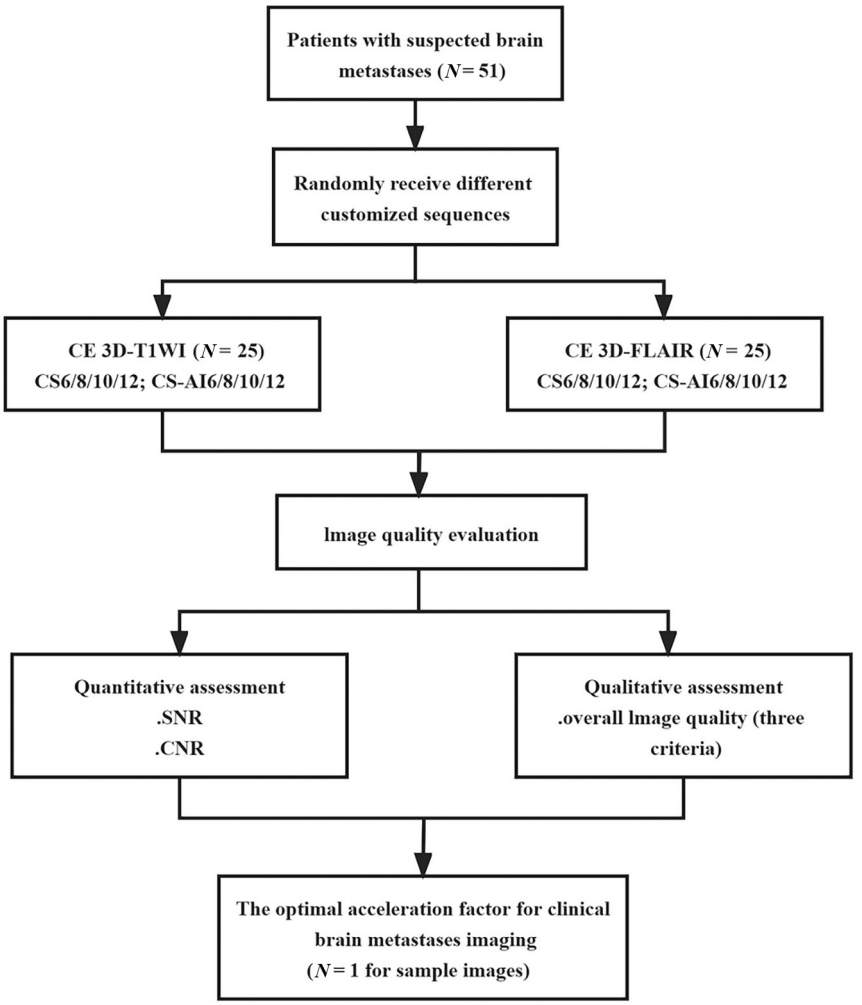

FIG 1. Flowchart of the experimental design.

image analyses. Regions of interest were placed on the lesion and adjacent normal white matter, avoiding areas of hemorrhage, necrosis, and vessels. The size of the delineated region of interest depended on the lesion size, ranging from 4.00 to 21.00 mm^2. To obtain comparable measurements, the area of interest first delineated on CS6 was copied and pasted in the corresponding regions on the images reconstructed via CS and CS-AI technology with different AFs. The standard deviation used to represent the noise and average signal intensity was recorded for each region of interest group. Based on the regions of interest, the SNR and contrast-to-noise ratio (CNR) were analyzed for objective evaluation by using Equations 1[20] and 2[21]:

$$1)\quad SNRlesion = \frac{SI_{lesion}}{SD_{lesion}}$$

$$2)\quad CNRlesion\_white\ matter = \frac{|SI_{lesion} - SI_{white\ matter}|}{\sqrt{SD_{lesion}{}^2 + SD_{white\ matter}{}^2}}$$

where SD stands for the standard deviation representing noise and SI represents the signal intensity.

Qualitative Image Analysis. All images were independently evaluated by 2 neuroradiologists (Y.M. and L.L.) with more than 15 years of experience and who were unaware of any clinical and sequence information. A 5-point Likert scale was used to grade the overall image quality: 1 = poor, nondiagnostic image quality; 2 = below average, interpretable but limited; 3 = average, interpretable; 4 = good; and 5 = excellent (including sharpness of gray-white matter boundaries, sharpness of lesion boundaries, and artifacts).[22] Subjective scores were independently assessed twice by 2 neuroradiologists, with the 2 readings separated by 4 weeks to avoid recall bias. The average value was used in a consistency test.

Statistical Analysis

All statistical analyses were performed using the GraphPad 9.5.1 (GraphPad Software) and MedCalc, version 19 (https://www.medcalc.org), statistical software packages. The interobserver consistency of the protocol images was calculated using a weighted Cohen kappa. The kappa value rating system was as follows: a kappa value of <0.2 indicated slight agreement; 0.21–0.40, fair agreement; 0.41–0.60, moderate agreement; 0.61–0.80, good agreement; and 0.81–1.00, excellent agreement.[23] The normality of quantitative parameters and subjective scores was analyzed using the Shapiro–Wilk test. The test results indicated that the SNR, CNR, and Likert scale scores were not normally distributed. Therefore, the Wilcoxon signed-rank test was used to compare the differences between the SNR, CNR, and subjective scores of the CS-AI protocols and CS at the same AF. The Friedman test was then used to compare the quantitative values of the images reconstructed by using the CS6 and CS-AI factors. In cases of statistical significance, the Dunn pairwise post hoc test was used to perform multiple comparisons. The threshold for statistical significance was set as $P < .05$.

RESULTS

Patient Characteristics

A total of 51 patients (27 men and 24 women; mean age, 57.22 ± 8.05 years; age range, 38–73 years) were included in this study. The primary malignancies included lung cancer ($n = 42$), breast cancer ($n = 6$), colon cancer ($n = 1$), malignant melanoma ($n = 1$), and kidney cancer ($n = 1$). Among them, 25 underwent accelerated CE 3D-T1WI by using the CS and CS-AI techniques, and a further 25 patients underwent CS- and CS-AI-accelerated CE

Table 1: Imaging parameters for CS- and CS-AI-accelerated CE 3D-T1WI sequences

Parameter	CE 3D-T1WI		
	CS6 (RS)	CS 8/10/12	CS-AI 6/8/10/12
TR (ms)	600	600	600
TE (ms)	28	28	28
FOV (mm^2)	250 × 250	250 × 250	250 × 250
Voxel size (mm^3)	0.99 × 1.00 × 1.10	0.99 × 1.00 × 1.10	0.99 × 1.00 × 1.10
Slices	327	327	327
Acceleration factor	6	8/10/12	6/8/10/12
Scan time (min)	3:34	2:42/2:10/1:49	3:34/2:42/2:10/1:49
Scan time reduction	-	24.29%/39.25%/49.06%	−/24.29%/39.25%/49.06%

Note:—dash indicates no value; RS, reference sequence; FOV, field of view; min, minute.

Table 2: Imaging parameters for CS- and CS-AI-accelerated CE 3D-FLAIR sequences

Parameter	CE 3D-FLAIR		
	CS6 (RS)	CS 8/10/12	CS-AI 6/8/10/12
TR (ms)	4800	4800	4800
TE (ms)	340	340	340
FOV (mm^2)	250 × 250	250 × 250	250 × 250
Voxel size (mm^3)	1.12 × 1.12 × 1.12	1.12 × 1.12 × 1.12	1.12 × 1.12 × 1.12
Slices	326	326	326
Acceleration factor	6	8/10/12	6/8/10/12
Scan time (min)	4:48	3:41/2:53/2:24	4:48/3:41/2:53/2:24
Scan time reduction	-	23.26%/39.93%/50.00%	-/23.26%/39.93%/50.00%

Note:—dash indicates no value; RS, reference sequence; FOV, field of view; min, minute.

3D-FLAIR imaging. After determining the optimal AF, 1 patient was scanned by using both optimized sequences.

Quantitative Assessment

Figure 2 shows the quantitative analysis results of the SNR and CNR for CS- and CS-AI-accelerated CE 3D-T1WI with different AFs. Under the same AF, the SNR and CNR of the CS-AI group were superior to those of the CS group (all $P < .05$), except at AF8, for which there was no statistically significant difference between the SNR values of the CS8 and CS-AI8 sequences ($P > .05$). Compared with the reference sequence CS6, the CS-AI groups had higher SNR and CNR values (all $P < .05$), with the CS-AI10 protocol showing the highest quantitative parameters.

Figure 3 shows the quantitative SNR and CNR analysis results for the CS and CS-AI-accelerated CE 3D-FLAIR images with different AFs. With the increase of the AF, the benefits of the CS-AI group continued up to AF10 (all $P < .05$) under the same AF conditions. At AF = 12, the SNR values of both CS and CS-AI decreased, and there was no statistical difference between the 2 groups ($P > .05$). Compared with the reference sequence CS6, the CS-AI groups exhibited significantly higher SNR and CNR values (all $P < .05$), with CS-AI10 being the most prominent.

In addition, for both the CE 3D-T1WI and CE 3D-FLAIR sequences, as the AF increased, the SNR and CNR of the images first increased and then decreased.

Qualitative Assessment

Between the 2 observers, the image scores of CE 3D-T1WI with different AFs were in good agreement [kappa (95% confidence interval) = 0.74 (0.68–0.80)], and the image scores of CE 3D-FLAIR were in excellent agreement [kappa (95% confidence interval) = 0.82 (0.77–0.87)]. Figure 4 shows that for both CE 3D-T1WI and CE 3D-FLAIR sequences, the image quality of the CS-AI group was superior to that of the CS group under the same AF (all $P < .05$). No statistically significant difference was observed in the overall image quality between the reference sequence CS6 and CS-AI12-accelerated CE 3D-T1WI ($P > .05$). In contrast, the image quality of all other CS-AI groups was superior to that of the reference sequence CS6 (all $P < .05$). Both neuroradiologists observed that CS-AI10 provided the best quality images ($P < .05$), with improved sharpness at the lesion boundaries and gray-white matter connections compared with the other acceleration protocols (Fig 5*C1*, *C2* and Fig 6*C1*, *C2*). Furthermore, in the CS group, as the AF increased, the gray-white matter junction of the CS10 and CS12 images became unsharp, boundaries of the lesions started becoming blurred, and artifact was more evident (Fig 5 and 6).

DISCUSSION

The clinical feasibility of CS-AI for the accelerated CE 3D-TIWI and CE 3D-FLAIR imaging of BM was investigated, and the optimal AF was explored by comparing CS and CS-AI technology with different AFs (6–12). Quantitative and qualitative assessments were used to analyze the acquired images to explore the value of applying CS-AI technology for patients with BM.

The quantitative analysis showed that the parameters of CE 3D-T1WI and CE-FLAIR reconstruction accelerated by CS-AI10 were superior to those of the other AF sequences. In the qualitative analysis, for the CE 3D-T1WI and CE 3D-FLAIR sequences, the image quality obtained by the CS-AI technique with different AFs was equal to or better than the overall image quality of the reference CS6, which indicated that the image quality obtained by the CS-AI protocol was at least comparable with that of the reference sequence. In addition, the 2 neuroradiologists observed that the CS-AI10-accelerated images improved the delineation of gray-white matter boundaries and lesion areas with better image quality than the other sequences. Therefore, when applying CS-AI technology to CE 3D-T1WI and CE 3D-FLAIR sequences on 3T MR systems and considering improving the image quality and shortening the scan time, AF10 is recommended. CS-AI exhibited higher CNR and better image quality at higher AFs, which may be attributed to its adaptive noise reduction capability. As the AF increases, the model's denoising effectiveness becomes more pronounced, resulting in images with enhanced contrast and improved image content, such as sharper gray-white matter connections and lesion

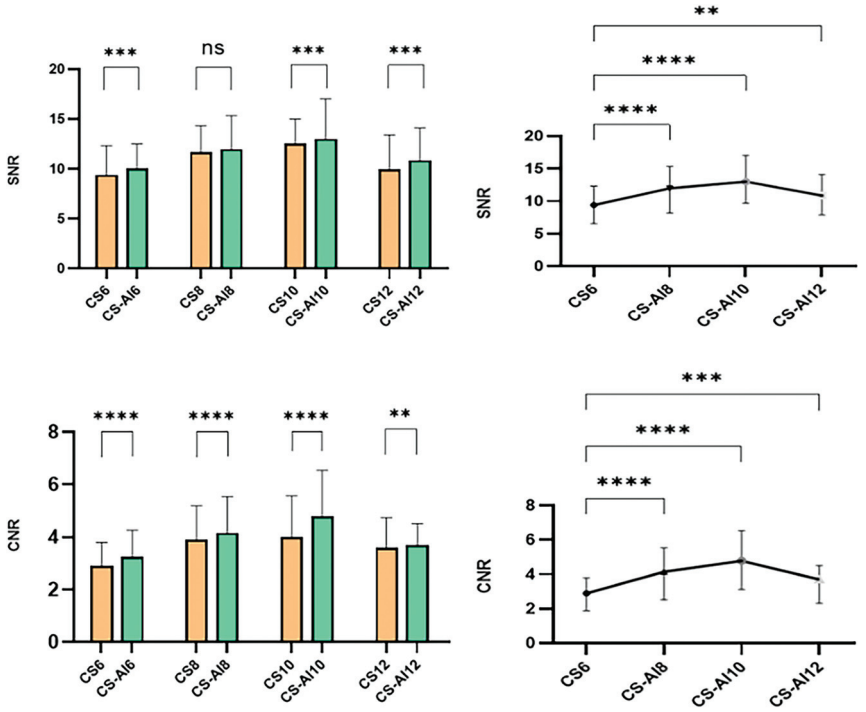

FIG 2. Quantitative analysis results of the SNR and CNR of CS- and CS-AI-accelerated CE 3D-T1WI under different AFs. Note: NS indicates not significant; *, $P < .05$; **, $P < .01$; ***, $P < .001$; ****, $P < .0001$.

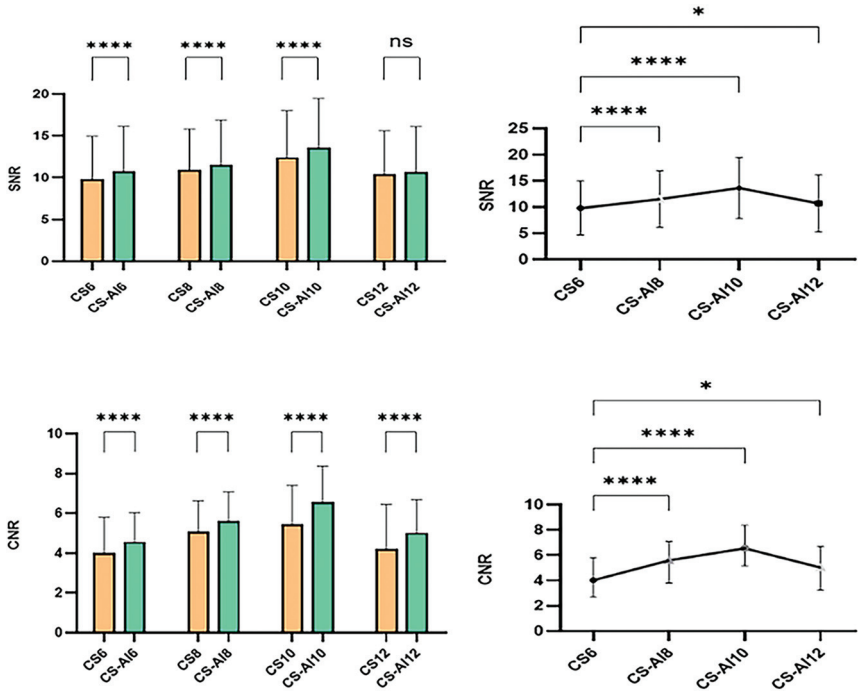

FIG 3. Quantitative analysis results of the SNR and CNR values of CS- and CS-AI-accelerated CE 3D-FLAIR images under different AFs. Note: NS indicates not significant; *, $P < .05$; **, $P < .01$; ***, $P < .001$; ****, $P < .0001$.

boundaries. However, there is a limit to denoising. When the level of undersampling is exceedingly high, even effective noise removal cannot fully compensate for the loss of image quality. The images tend to become blurred, and critical details are often lost, which adversely affects the diagnostic quality of these images. These phenomena are supported by our subjective scores.

CE-T1WI and CE-FLAIR sequences play essential roles in detecting BM. Some studies have shown that CE-T1WI sequences

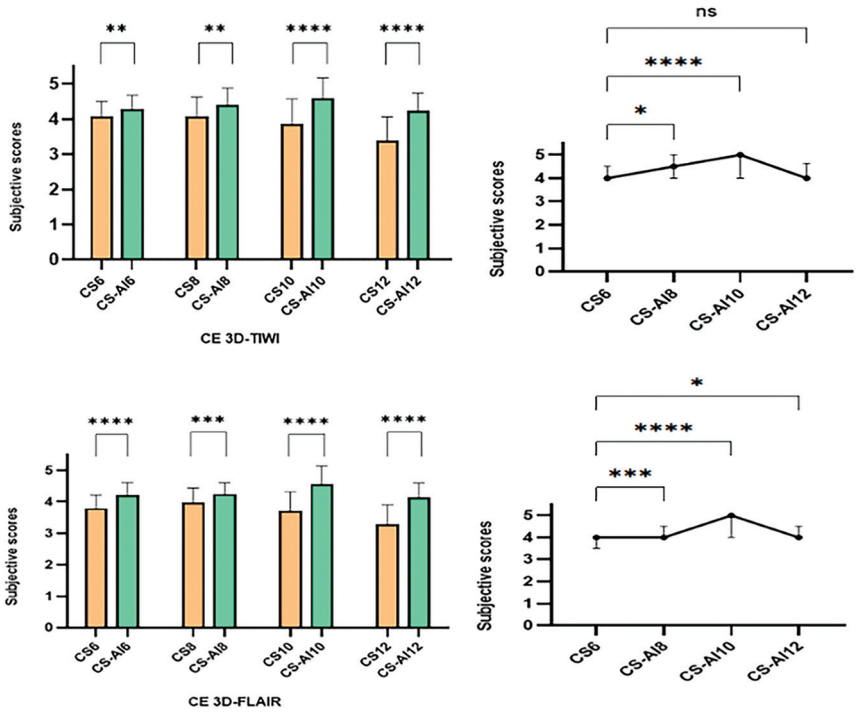

FIG 4. Comparison of the overall image quality score results of different accelerated sequences in patients with BM. Note: NS indicates not significant; *, $P < .05$; **, $P < .01$; ***, $P < .001$; ****, $P < .0001$.

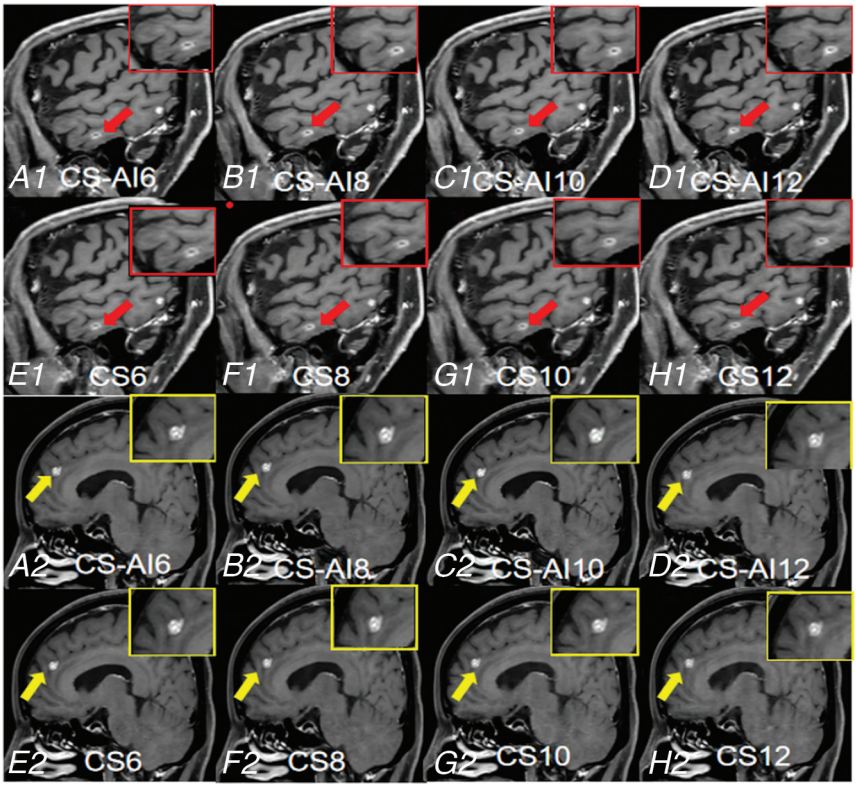

FIG 5. MR images of a 68-year-old woman with breast cancer and a 57-year-old man with lung cancer. Reconstructed CE 3D-T1-weighted sagittal images for CS-AI6 (*A1, A2*), CS-AI8 (*B1, B2*), CS-AI10 (*C1, C2*), CS-AI12 (*D1, D2*), reference CS6 (*E1, E2*), CS8 (*F1, F2*), CS10 (*G1, G2*), and CS12 (*H1, H2*). The arrows indicate enhanced BM lesions. Notably, the gray-white matter boundaries and lesion edges are clearer in the images accelerated by CS-AI technology, and the image quality is comparable with or better than that of CS6.

clearly show lesions in the brain parenchyma, whereas the CE-FLAIR sequence is more likely to detect BM on the surface of the cerebral cortex and leptomeningeal metastases and to help distinguish small lesions from cerebral vessels.[24,25] In addition, 3D sequences with higher spatial resolution are more advantageous for detecting small metastatic lesions when evaluating BM because 3D sequences can perform multiplanar reconstruction and reduce the partial volume effect compared with 2D sequences. However, the disadvantage of a 3D scan is that a longer scan time is required. Increasing scan times can be challenging for some patients, leading to possible image artifacts and even complete scan failures. Furthermore, longer acquisition times can increase the costs of clinical examinations by reducing patient throughput.[26]

Various MR imaging acceleration techniques have been developed to reduce image acquisition and reconstruction times, among which parallel imaging and compressed sensing are the most influential. Both methods improve the scanning speed by undersampling the *k*-space. However, the larger the AF of parallel imaging, the

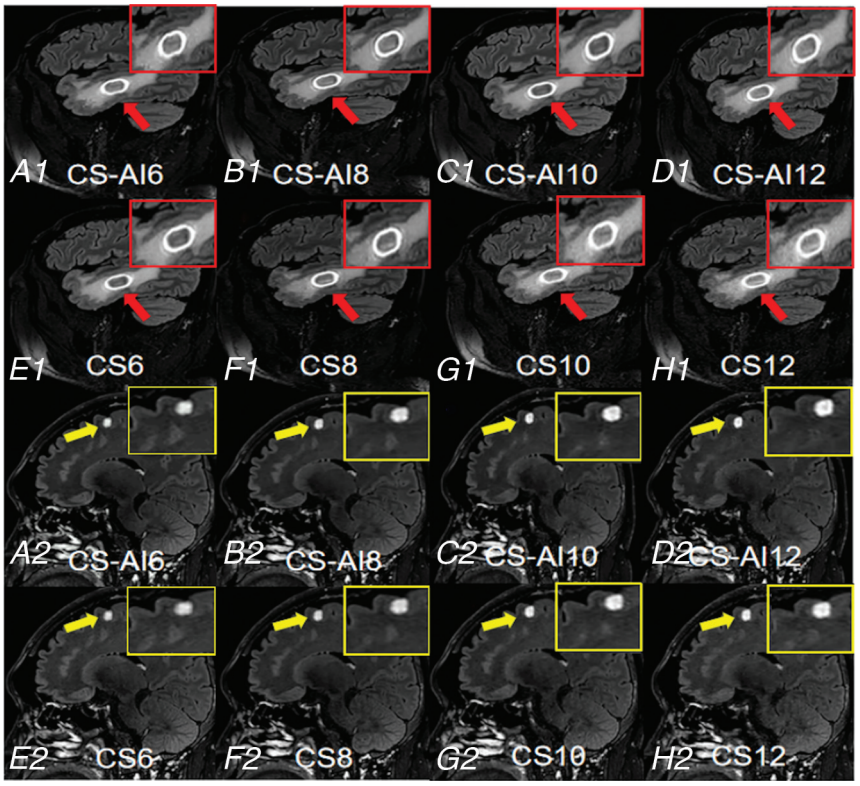

FIG 6. MR images of a 55-year-old male patient and a 38-year-old male patient with lung cancer. Reconstructed CE 3D-FLAIR sagittal images for CS-AI6 (*A1, A2*), CS-AI8 (*B1, B2*), CS-AI10 (*C1, C2*), CS-AI12 (*D1, D2*), reference CS6 (*E1, E2*), CS8 (*F1, F2*), CS10 (*G1, G2*), and CS12 (*H1, H2*). The arrows indicate enhanced BM. In the CS group, as the AF increases, the images become blurred, and the junctions of gray-white matter and the boundaries of the lesions become less clear.

lower the SNR of the image and the easier it is to produce fold-over artifacts. Though CS is superior to conventional SENSE-type parallel imaging in maintaining SNR and is less prone to generating artifacts, the image quality often degrades due to insufficient noise removal when the AF is higher than a certain level.[27] In this study, the CS group exhibited lower overall image quality scores for CS12-accelerated CE 3D-T1WI and CE 3D-FLAIR sequences compared with other AFs. Addressing these problems by applying a deep learning framework in the original data reconstruction is expected to reduce the scanning time while preserving image quality.

Deep learning is a popular machine learning approach that can automatically extract features and process high-dimensional medical image data.[28] Currently, this is the most widely used AI approach for medical images. One of its primary applications in medical imaging is accelerated MR imaging.[29,30] Recently, researchers have applied this method to sequence optimization. For instance, Park et al[31] demonstrated that fast MR imaging based on deep learning can be used to reduce the acquisition time of prostate MR imaging without compromising diagnostic performance. Zhao et al[32] used AI-assisted CS technology to accelerate T2-weighted kidney imaging, which obviously shortened the scanning time, and the image quality was equal to or better than that of traditional technology. Sheng et al[33] used a convolutional neural network framework to improve the reconstruction speed and image quality of single breath-hold T2-weighted sequences in liver scanning. This implies that image reconstruction functions in AI can further enhance the clinical applicability of time-consuming imaging sequences.

To our knowledge, this is the first study to comprehensively evaluate CS-AI for the imaging of patients with BM. Vranic et al[7] used CS to accelerate 3D sequence scanning in patients with brain tumors. However, that study utilized only 1 specific AF. While the findings underscore the superiority of CS over traditional scanning methods, the research did not determine the optimal AF, indicating a need for further exploration in this area. Zhang et al[34] evaluated the feasibility of CS with different AFs for the imaging of patients with brain tumors, but this was done only for 3D amide proton transfer-weighted sequences, and they concluded by recommending CS4. In this study, we obtained corresponding images for objective and subjective evaluations by applying CS and CS-AI to patients with BM and explored the optimal AF for clinical BM imaging. Notably, in this study, though the SNR and CNR of CS12 were better than or roughly similar to those of CS6, the image quality obtained after the reconstruction of the 2 sequences was inferior to that of CS6 (Fig 5 *H1, H2*; and Fig 6 *H1, H2*). This indicated that the quantitative parameters did not fully represent the overall image quality in terms of iterative image reconstruction and denoising. Objective and subjective evaluations must be combined to comprehensively analyze image diagnostic performance.

This study has some limitations. First, this was a single-center prospective study with a small sample size that exclusively used single vendor equipment. Due to the incompatibility of CS-AI with other manufacturers' devices, its applicability is restricted to Philips MR imaging systems. In addition, the study did not explore the use of this technology with various MR imaging coils or lower field strength systems, nor did it explore its generalizability to similar equipment in different hospital settings. Therefore, future research should consider these aspects to further enhance the understanding and application of CS-AI in various MR imaging contexts. Second, BM were mainly confirmed during follow-ups. Patients with multiple BM frequently do not undergo surgery, so lesions are rarely pathologically confirmed. Third, CS- or CS-AI-accelerated scans with different AFs were performed in a random acquisition order to reduce time bias. This may have influenced the enhancement of the lesions to some extent; however, the 2 raters considered no significant difference in enhancement between the observed images. Finally, 42 of the 51 patients included in this study had lung cancer. Theoretically, these findings can only be applied to BM due to

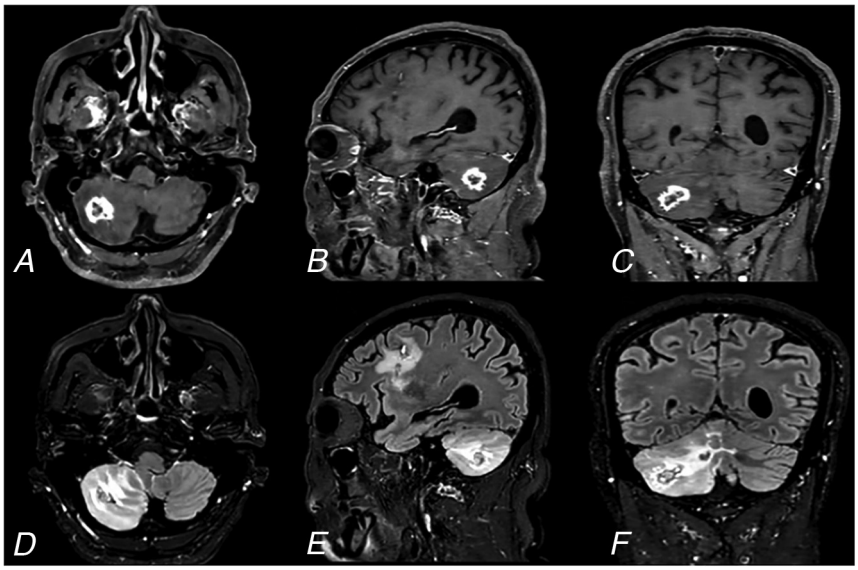

FIG 7. A 60-year-old male patient with lung cancer was scanned with 2 optimized sequences to obtain example images of a good quality in a short time (5:03 minutes). The axial (*A*), sagittal (*B*), and coronal (*C*) images of accelerated CE 3D-T1Wl of CS-AI10. The axial (*D*), sagittal (*E*), and coronal (*F*) images of accelerated CE 3D-FLAIR of CS-AI10.

lung cancer. Therefore, more heterogeneous populations are needed to confirm these results in patients with other metastatic tumors.

CONCLUSIONS

Combining CS and deep learning can shorten scanning time while maintaining or improving image quality compared with conventional CS. Using CS-AI with AFs up to 10 to reconstruct CE 3D-T1WI and CE 3D-FLAIR sequences on a 3T MR machine could reduce scanning time and improve diagnostic performance. When CS-AI10 (Fig 7) was used for acceleration, CE 3D-T1WI and CE 3D-FLAIR sequences were 39.25% (2:10 minutes versus 3:34 minutes) and 39.93% (2:53 minutes versus 4:48 minutes) faster than CS6, respectively. The use of CS-AI technology could optimize CE 3D scans when performing clinical imaging of patients with BM to help radiologists better evaluate lesions in detail while improving scanning efficiency.

Disclosure forms provided by the authors are available with the full text and PDF of this article at www.ajnr.org.

REFERENCES

1. Kaufmann TJ, Smits M, Boxerman J, et al. **Consensus recommendations for a standardized brain tumor imaging protocol for clinical trials in brain metastases.** *Neuro Oncol* 2020;22:757–72 CrossRef Medline
2. Li R, Guo Y, Zhao Z, et al. **MRI-based two-stage deep learning model for automatic detection and segmentation of brain metastases.** *Eur Radiology* 2023;33:3521–31 CrossRef Medline
3. Derks SH, van der Veldt AA, Smits M. **Brain metastases: the role of clinical imaging.** *Br J Radiology* 2022;95:20210944 CrossRef Medline
4. Villanueva-Meyer JE, Mabray MC, Cha S. **Current clinical brain tumor imaging.** *Neurosurgery* 2017;81:397–415 CrossRef Medline
5. Kim D, Heo YJ, Jeong HW, et al. **Usefulness of the delay alternating with nutation for tailored excitation pulse with T1-weighted sampling perfection with application-optimized contrasts using different flip angle evolution in the detection of cerebral metastases: Comparison with MPRAGE imaging.** *AJNR Am J Neuroradiol* 2019;40:1469–75 CrossRef Medline
6. Langer CJ, Mehta MP. **Current management of brain metastases, with a focus on systemic options.** *J Clin Oncol* 2005;23:6207–19 CrossRef Medline
7. Vranic JE, Cross NM, Wang Y, et al. **Compressed sensing-sensitivity encoding (CS-SENSE) accelerated brain imaging: reduced scan time without reduced image quality.** *AJNR Am J Neuroradiol* 2019;40:92–98 CrossRef Medline
8. Duan Y, Zhang J, Zhuo Z, et al. **Accelerating brain 3D T1-weighted turbo field echo MRI using compressed sensing-sensitivity encoding (CS-SENSE).** *Eur J Radiology* 2020;131:109255 CrossRef Medline
9. Sasi SD, Ramaniharan AK, Bhattacharjee R, et al. **Evaluating feasibility of high resolution T1-perfusion MRI with whole brain coverage using compressed SENSE: Application to glioma grading.** *Eur J Radiology* 2020;129:109049 CrossRef Medline
10. Boyarko AC, Dillman JR, Tkach JA, et al. **Comparison of compressed SENSE and SENSE for quantitative liver MRI in children and young adults.** *Abdom Radiology (NY)* 2021;46:4567–75 CrossRef Medline
11. Cho SJ, Choi YJ, Chung SR, et al. **High-resolution MRI using compressed sensing-sensitivity encoding (CS-SENSE) for patients with suspected neurovascular compression syndrome: comparison with the conventional SENSE parallel acquisition technique.** *Clin Radiology* 2019;74:817.e9–e14 CrossRef Medline
12. Hsiao A, Lustig M, Alley MT, et al. **Evaluation of valvular insufficiency and shunts with parallel-imaging compressed-sensing 4D phase-contrast MR imaging with stereoscopic 3D velocity-fusion volume-rendered visualization.** *Radiology* 2012;265:87–95 CrossRef Medline
13. Knoll F, Zbontar J, Sriram A, et al. **fastMRI: A publicly available raw k-Space and DICOM dataset of knee images for accelerated MR image reconstruction using machine learning.** *Radiology Artif Intell* 2020;2:e190007 CrossRef Medline
14. Knoll F, Murrell T, Sriram A, et al. **Advancing machine learning for MR image reconstruction with an open competition: Overview of the 2019 fastMRI challenge.** *Magn Reson Med* 2020;84:3054–70 CrossRef Medline
15. Pezzotti N, Yousefi S, Elmahdy MS, et al. **An adaptive intelligence algorithm for undersampled knee MRI reconstruction.** *IEEE Access* 2020;8:204825–38 CrossRef
16. Foreman SC, Neumann J, Han J, et al. **Deep learning-based acceleration of compressed sense MR imaging of the ankle.** *Eur Radiology* 2022;32:8376–85 CrossRef Medline
17. Fervers P, Zaeske C, Rauen P, et al. **Conventional and deep-learning-based image reconstructions of undersampled K-space data of the lumbar spine using compressed sensing in MRI: A comparative study on 20 subjects.** *Diagnostics (Basel)* 2023;13:418 CrossRef Medline
18. Dratsch T, Siedek F, Zäske C, et al. **Reconstruction of shoulder MRI using deep learning and compressed sensing: a validation study on healthy volunteers**. *Eur Radiology Exp* 2023;7:66 CrossRef Medline
19. Ni M, He M, Yang Y, et al. **Application research of AI-assisted compressed sensing technology in MRI scanning of the knee joint: 3D-MRI perspective.** *Eur Radiology* 2023 CrossRef Medline
20. Dietrich O, Raya JG, Reeder SB, et al. **Measurement of signal-to-noise ratios in MR images: influence of multichannel coils, parallel**

imaging, and reconstruction filters. *J Magn Reson Imaging* 2007;26:375–85 CrossRef Medline
21. Kakeda S, Korogi Y, Hiai Y, et al. **Detection of brain metastasis at 3T: comparison among SE, IR-FSE and 3D-GRE sequences.** *Eur Radiology* 2007;17:2345–51 CrossRef Medline
22. Conklin J, Longo MGF, Cauley SF, et al. **Validation of highly accelerated wave-CAIPI SWI compared with conventional SWI and T2*-weighted gradient recalled-echo for routine clinical brain MRI at 3T**. *AJNR Am J Neuroradiol* 2019;40:2073–80 CrossRef Medline
23. Chung MS, Yim Y, Sung JK, et al. **CS-VIBE accelerates cranial nerve MR imaging for the diagnosis of facial neuritis: comparison of the diagnostic performance of post-contrast MPRAGE and CS-VIBE.** *Eur Radiology* 2022;32:223–33 CrossRef Medline
24. Jin T, Zhang H, Liu X, et al. **Enhancement degree of brain metastases: correlation analysis between enhanced T2 FLAIR and vascular permeability parameters of dynamic contrast-enhanced MRI.** *Eur Radiology* 2021;31:5595–604 CrossRef Medline
25. Ercan N, Gultekin S, Celik H, et al. **Diagnostic value of contrast-enhanced fluid-attenuated inversion recovery MR imaging of intracranial metastases.** *AJNR Am J Neuroradiol* 2004;25:761–65 Medline
26. Toledano-Massiah S, Sayadi A, de Boer R, et al. **Accuracy of the compressed sensing accelerated 3D-FLAIR sequence for the detection of MS plaques at 3T.** *AJNR Am J Neuroradiol* 2018;39:454–58 CrossRef Medline
27. Dieckmeyer M, Roy AG, Senapati J, et al. **Effect of MRI acquisition acceleration via compressed sensing and parallel imaging on brain volumetry.** *MAGMA* 2021;34:487–97 CrossRef Medline
28. Schlemper J, Caballero J, Hajnal JV, et al. **A deep cascade of convolutional neural networks for dynamic MR image reconstruction.** *IEEE Trans Med Imaging* 2018;37:491–503 CrossRef Medline
29. Gu H, Yaman B, Moeller S, et al. **Revisiting [Formula: see text]-wavelet compressed-sensing MRI in the era of deep learning.** *Proc Natl Acad Sci U S A* 2022;119:e2201062119 CrossRef Medline
30. Bash S, Wang L, Airriess C, et al. **Deep learning enables 60% accelerated volumetric brain MRI while preserving quantitative performance: A prospective, multicenter, multireader trial**. *AJNR Am J Neuroradiol* 2021;42:2130–37 CrossRef Medline
31. Park JC, Park KJ, Park MY, et al. **Fast T2-weighted imaging with deep learning-based reconstruction: Evaluation of image quality and diagnostic performance in patients undergoing radical prostatectomy.** *J Magn Reson Imaging* 2022;55:1735–44 CrossRef Medline
32. Zhao Y, Peng C, Wang S, et al. **The feasibility investigation of AI-assisted compressed sensing in kidney MR imaging: an ultra-fast T2WI imaging technology.** *BMC Med Imaging* 2022;22:119 CrossRef Medline
33. Sheng RF, Zheng LY, Jin KP, et al. **Single-breath-hold T2WI liver MRI with deep learning-based reconstruction: A clinical feasibility study in comparison to conventional multi-breath-hold T2WI liver MRI.** *Magn Reson Imaging* 2021;81:75–81 CrossRef Medline
34. Zhang N, Zhang H, Gao B, et al. **3D amide proton transfer weighted brain tumor imaging with compressed SENSE: Effects of different acceleration factors.** *Front Neurosci* 2022;16:876587 CrossRef Medline